Nanoscale

Accepted Manuscript

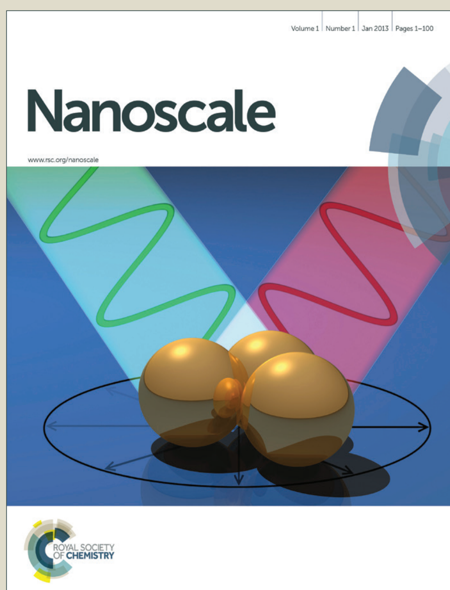

This is an *Accepted Manuscript*, which has been through the Royal Society of Chemistry peer review process and has been accepted for publication.

Accepted Manuscripts are published online shortly after acceptance, before technical editing, formatting and proof reading. Using this free service, authors can make their results available to the community, in citable form, before we publish the edited article. We will replace this *Accepted Manuscript* with the edited and formatted *Advance Article* as soon as it is available.

You can find more information about *Accepted Manuscripts* in the Information for Authors.

Please note that technical editing may introduce minor changes to the text and/or graphics, which may alter content. The journal's standard Terms & Conditions and the Ethical guidelines still apply. In no event shall the Royal Society of Chemistry be held responsible for any errors or omissions in this *Accepted Manuscript* or any consequences arising from the use of any information it contains.

ROYAL SOCIETY OF CHEMISTRY

www.rsc.org/nanoscale

Cite this: DOI: 10.1039/c0xx00000x

www.rsc.org/xxxxxx

ARTICLE TYPE

Si microstructures laminated with nanolayer of TiO_2 as long-term stable and effective photocathodes in PEC devices

Chittaranjan Das,*[a] Massimo Tallarida[a] and Dieter Schmeisser[a]

Received (in XXX, XXX) Xth XXXXXXXXX 20XX, Accepted Xth XXXXXXXXX 20XX
DOI: 10.1039/b000000x

Photoelectrochemical (PEC) water splitting is one of the most emerging fields for green energy generation and storage. Here we show a study of microstructured Si covered by TiO_2 nano-layer. The microstructures are prepared by Galvanostatic selective etching of Si. The TiO_2 nano-layer was deposited by atomic layer deposition (ALD) to protect the microstructured photocathode against corrosion. The obtained microstructured photocathode showed a shift in onset potential of 400mV towards anodic direction compared to bare Si. The Si microstructures laminated with nano-layer of TiO_2 shows stability over 60 hours of measurement.

Introduction

Photoelectrochemical (PEC) water splitting is one of the most emerging fields for green energy generation and storage. PEC devices can be fabricated using semiconducting materials for photocatalytic water splitting. But for this purpose, the semiconductor must have an appropriate band gap around 1.7eV and a right band edge position with respect to the water oxidation and reduction potentials[1]. Presently, the semiconducting materials satisfy the above conditions only partially, and efficient PEC devices need a tandem-cell design. In this case, Si is one of the most promising materials for the tandem-cell PEC devices, although it has low band gap. In fact, Si has a band gap of 1.1eV and can absorb within the visible range of the light but it can produce a maximum photovoltage of 450mV.

In addition, Si has distinct problems in PEC devices, such as photoelectrochemical corrosion or low quantum yield. The p-type Si is considerably more stable against photooxidation than the n-type counterpart but it has a lower quantum yield (QY). Also, its high reflectance is typically an issue. The QY of p-type Si can be increased by a surface modification, e.g. by using a catalyst, while reflectance can be reduced by a surface structuring.

In both n- and p-type Si, self-oxidation of surface in aqueous electrochemical media occurs. In non-aqueous medium, instead, Si has a lower photovoltage due to the small band bending at the redox level of the electrolyte. To overcome these limitations usually an external potential is applied.

The catalytic activity of both n- and p-type Si can be increased by using various catalysts for either water oxidation or reduction on either n- or p-type Si, respectively. Noble catalyst materials such as Pt or Pd are typically used for hydrogen evolution reaction (HER) on Si. More recently, MoS_2, Ni-Mo and Ni-Co [2] alloys have been successfully used as well. For oxygen evolution reaction (OER) on Si, the typical catalysts were Pt, RuO_2, IrO, Co_2O_3 [3].

Another problem arising in PEC devices based on planar Si electrodes is the high reflectivity which reduces the light absorption and leads to a lower efficiency. Absorption may be also reduced by the loading of catalyst onto the Si surface because of the scattering of the light on the catalyst surface.

It was demonstrated that the reflectance can be decreased, and consequently the light collection can be increased, by structuring the silicon surface, bringing to an overall increase the efficiency of Si photocathodes. It was also reported that structured p-type Si photocathodes present an increased onset potential towards anodic direction [4]. The synthesis of nanostructure needs lithography or catalyst based etching in the top down method and catalyst based CVD deposition in bottom up method. Both of these methods are multi step and each step is critical to control.

In this work, we demonstrate a cost-effective and a single-step etching process to enhance the Si photoelectrochemical activity. In particular, the electrochemical (catalyst-less) etching process of p-Si which can produce a reproducible and efficient microstructuring of the Si surface with a formation of Si micropillars (SiMPs) will be shown. Such prepared SiMPs show a higher photocurrent density than the planar Si and a shift in the onset potential towards anodic direction. Moreover, the conformal cover of the SiMPs by a highly conductive [5] and conformal [6] thin atomic layer deposited (ALD) TiO_2 overlayer will be presented.

Experimental

A p-type Si(100) wafer with a resistivity of $10^{-20}\Omega$cm from the CrysTec GmbH was taken as a substrate for etching. It was cut into pieces of $1\times1cm^2$ and prior to the electrochemical etching the Si pieces were sonicated for 5min in each of the following solutions: isopropanol, acetone and deionized water using an ultrasonic bath. The electrochemical etching solution is prepared by taking a mixture of HF(48%)-C_2H_5OH(99%)-H_2O in 1:1:2 volume [7]. A single compartment, two electrode system was used for electrochemical etching. The electrochemical etching was

Nanoscale Accepted Manuscript

carried out in a galvanostatic mode by applying a current density starting from $2mA/cm^2$ to $40mA/cm^2$ for different etching times with a KEITHLEY system. The preparations of microstructured Si were carried out in a fume hood to avoid contaminations from the electrochemical system during etching.

The surface morphology of the etched samples was characterized by scanning electron microscope (SEM). To determine the elemental composition of these structures X-ray photoelectron spectroscopy (XPS) was carried out by using Omicron XPS system. Mg Kα X-ray source with energy of 1253eV was used.

The photoelectrochemical activity of the Si electrodes was investigated by using a VERSTAT4 potentiostat with a three electrode bottom cell electrochemical setup. As electrolyte an 0.1M H_2SO_4 was used and Ag/AgCl and Pt foil were applied as reference and counter electrodes, respectively. The scan rates for CV and j-V measurements were 50mV/sec. A visible light source from Euromex Illuminator EK 1 with an intensity of $40mW/cm^2$ and the wavelength of 580nm was used for the photoelectrochemical measurements. The lamp has tungsten filament.

A shower head-type, laboratory-built ALD system was used to deposit a TiO_2 thin film[7]. A titanium isopropoxide (TTIP) was used as a source of Ti and water as a source of O_2. The pulse time for TTIP was 4sec and for water 0.5sec. The time interval between two consecutive cycles was 10sec. The substrate temperature was 250 ℃ and the pressure in the range of 10^{-6}mbar.

Results and discussion

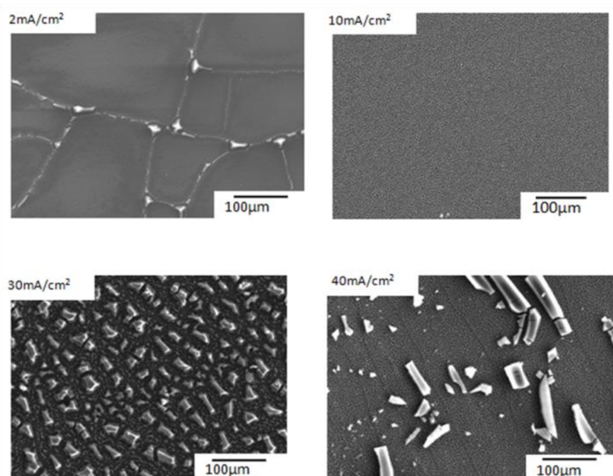

Fig. 1 Scanning electron microscopy (SEM) images of the Si substrate after 30 minutes of etching in a galvanostatic mode by applying current densities of $2mA/cm^2$ (a), $10mA/cm^2$ (b), $30mA/cm^2$ (c) and $40mA/cm^2$ (d).

The electrochemical etching was carried out in a galvanostatic mode in a mixture of HF(48%)-C_2H_5OH(99%)-H_2O in a volume relation of 1:1:2. The formation of pores or microstructures consists of two processes: (1) an electrochemical step and (2) a chemical step[8] . In the electrochemical step the formation of SiF_2 takes place, followed by the formation of SiO_x. The SiO_x film is subsequently removed in the chemical step. This process flow is illustrated in Fig. 1 (a-d), where the morphology of samples treated with increasing galvanostatic current density are shown.

At low current density the formation of SiO_x is dominated and the etching process is limited, whereas at high current density both, the formation of the SiF_2-SiO_x layer and the etching occur simultaneously and form pillar-like structures. In fact, the surface etched with a $2mA/cm^2$ of current density shows only small cracks (Fig.1a), while for higher value of applied current density the formation of micropores on the Si surface appears (Fig. 1(b)-(d)).

It has been shown, that when the applied current density is higher than $20mA/cm^2$ the Si pores start to form[8]. In our case, the pores formation has been observed already at $10mA/cm^2$ of a current density, as shown in Fig. 1(b), but the pores were always covered with a thick initiation layer. The slow rate of dissolution of the initiation layer at this current density hinders the formation of the pillar-like structures. Therefore, to prepare SiMPs with different thicknesses we selected a current density of $40mA/cm^2$ for etching and we changed the etching time.

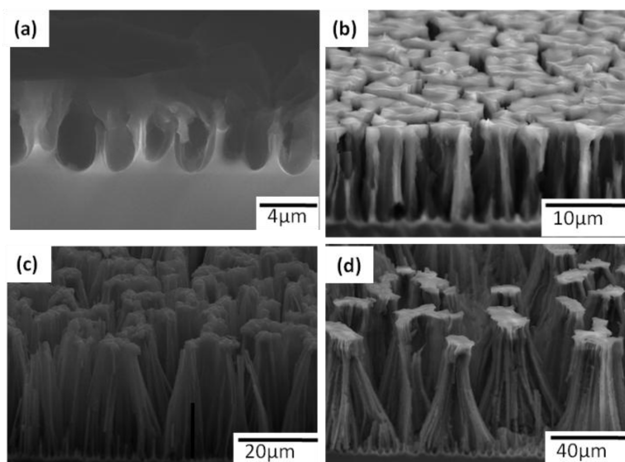

Fig. 2 Cross-sectional SEM image of the microstructured Si etched with a current density of $40mA/cm^2$ for 5min (a), 10min (b), 20min (c) and 30min (d). Is should be noticed that the scale bars in the images are not the same, so the reader should consider the increase in magnification bar.

The thickness of the structured layers indeed increased with the etching time at a constant applied current density. In Fig. 2(a), after 5min of etching the surface of Si is covered with a thick initiation layer and underneath micropillars are formed. While increasing the etching time, the initiation layer is also etched and the thickness of the SiMPs increases due to the anisotropic etching. After etching for 10min the initiation layer is still present on the surface (Fig. 2(b)), but after 20min of etching the initiation layer is completely removed, as can be seen in Fig. 2(c) and 2(d). When the etching time is increased to 60min, the height of the microstructured Si pillars increases further and they cannot stand freely and they collapse.

Nanoscale Accepted Manuscript

This journal is © The Royal Society of Chemistry [year]

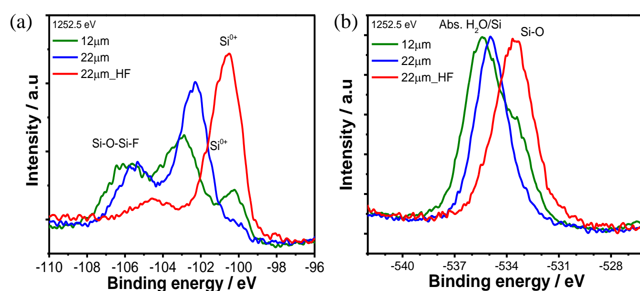

Fig. 3 Si 2p (a) and O 1s (b) XPS core levels of the 12 μm, 22 μm, and etched by HF 22 μm thick as grown samples. The O 1s spectra are normalized to the same maximum intensity to show evidence in the different peak position, while the Si 2p spectra are not modified.

The Si 2p core level XPS spectra of the 12, 22 and 22 μm_HF SiMPs samples are shown in Fig. 3(a). The two peaks located at around 102.8 and 106 eV in the 12μm sample spectrum can be attributed to SiO_2 and Si-OH/Si-F components, respectively. Due to the formation of SiO_2 and Si-OH/Si-F on the sample surface the signal from the metallic silicon (Si^0 at binding energy of 100eV) is attenuated. Therefore, it can be concluded that the 1.5μm thick initiation layer of the 12μm sample consists of SiO_2, Si-OH/Si-F and non-reacted Si.

The 22μm SiMPs sample has two distinct peaks in the Si 2p XPS spectrum at around 102 and 105.7eV with a clear shoulder at 100eV. The peak at 102eV could be due to differential charging of the Si underneath the SiO_2 and Si-OH/Si-F covering, while the peak at 105.7eV could be due to SiO_2 with little amount of Si-OH/Si-F. Therefore, it can be concluded that for longer electrochemical etching time the initiation layer is only partially removed and the Si micropillars are still covered by SiO_2 and Si-OH/Si-F.

To identify whether the micropillars, shown in Fig. 3(c), consist of pure Si or of SiO_2 and/or Si-OH/Si-F, the 22μm sample was etched with HF and the Si 2p XPS spectrum (22μm_HF) was collected. It can be seen, that the HF etching procedure successfully removed the SiO_2 and/or Si-OH/Si-F (broad peak at around 105eV) initiation layer and that the micropillars consist of metallic Si (high intense peak at 100eV in the 22μm_HF spectrum).

The Si 2p XPS results are further confirmed by the O 1s XPS spectra, shown in Fig. 3(b). The O 1s core level spectra of the 12 and 22μm samples consist of two main peaks at around 533.3 and 535eV, which can be attributed to Si-O and absorbed H_2O [9, 10]. However, after the etching procedure with HF the adsorbed H_2O is removed and the O 1s spectrum shows only a single peak at 533.3eV which corresponds to the remaining SiO_2 on the Si microstructure surface.

Therefore, it can be concluded, that the longer electrochemical etching time not only increases the height of the mircopillars, but also removes more effectively the initiation layer consisting of SiO_2 and/or Si-OH/Si-F; and that this initial layer can be successfully removed by the HF etching.

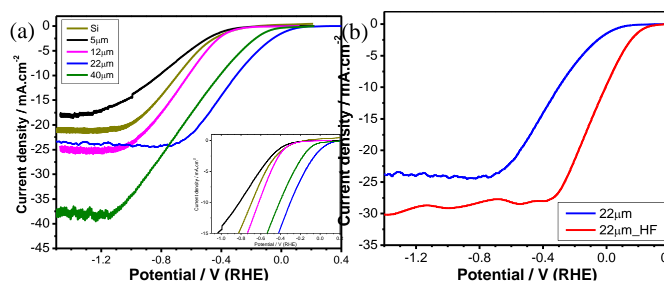

Fig.4 Photoelectrochemical activity (density of current vs. voltage (j-V) characteristics) (a) of the planar and microstuctured Si photocathodes prepared with pillars of different thickness to check the H_2 production performance under visible light irradiation in 0.5M sulfuric acid, and (b) of the microstructured Si samples before and after HF etching.

The photocurrent density vs. voltage (j-V) graph in Fig. 4 shows the performance in 0.1M sulfuric acid electrolyte of the planar Si and SiMPs photocathodes having different thickness. In the j-V curve the photocurrent of Si starts to change at around -400mV (RHE) and reaches saturation at around -1V (RHE). The SiMPs photocathodes show the same behavior but in most of the SiMPs photocathodes, with the exception of the 5 μm thick sample, the photocurrent starts at more positive voltages than that in the bare Si photocathode. Although the onset potential of bare Si and the 12 μm are same, the photocurrent density and the slope of the curve that represents the reaction kinetics are better in the 12 μm SiMPs as can be seen in the onset of Fig. 4(a). Apparently in the 5 μm thick SiMPs photocathode, the photocurrent starts at more negative voltage compared to bare Si, and the saturation photocurrent density of the 5 μm SiMPs photocathode is smaller than the bare Si.

The increase of the photocurrent density and the shift in onset potential towards anodic direction shows the improvement in the electrochemical performance of the SiMPs when a thickness larger than 5 μm is used. However, we observed that the diameter of the pillars is similar (~1 μm) in all the SiMPs samples, and only their height is different. Therefore, we tentatively suggest that the photoelectrochemical performance depends on the height of the pillars.

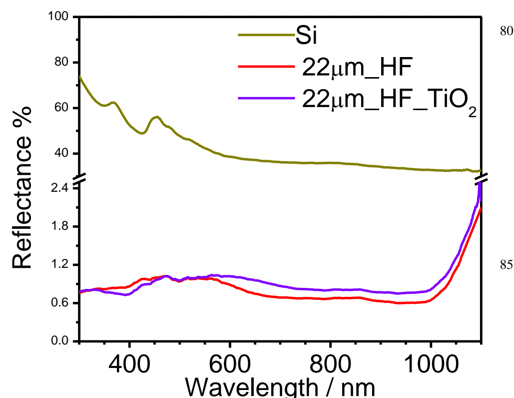

Fig.5 Optical reflectance of planar Si, 22μm_HF and 22μm_HF_TiO_2 photocathodes in the wavelength range from 300 to 1100 nm.

In our setup, we found that the saturation current density of

Nanoscale Accepted Manuscript

the planar Si is about 21mA/cm^2 whereas for the 5, 12, 22 and 40μm thick SiMPs it displayed values of 18, 25, 24 and 37.5mA/cm^2, respectively (Fig. 4(a)). The difference in the saturation photocurrent could be related to the surface reflectance as well as the surface area of the photocathodes. Indeed, the planar Si electrode is expected to have a higher surface reflectance of the incident light of about 25%[11], at the Si-water interface. To indentify the difference in reflectance of planar Si and the SiMPs we performed UV-Visible spectroscopy using total hemispherical reflectance mode, as shown in Fig.5. In the total visible photon energy range the SiMPs have lower reflectance in comparison to planar Si. At the wavelength of 580 nm the planar Si has a reflectance of 39.5% while for SiMPs of 22um_HF it is only about 1%. The lamination of TiO_2 ALD layer on the SiMPs does not influence the reflectance. The reduction of the surface reflectance increases the current density due to the higher absorption and hence the quantum efficiency also increases. For example, the photoabsorption property of microstructures is discussed in the literature in terms of enhanced light trapping that enhances the photocurrent of nanostructured Si[12,13]. The microstructures here have rough surfaces and poor surface properties compared to planar Si. But the microstructuring decreases the surface reflectance (Fig.5) of the Si and increases the surface area of the photoelectrode. The increase in surface area and surface absorption is reflected in the J-V measurements and SiMPs have better photoresponse and more positive onset potential (Fig.4). Also SiMPs with diameters of around 1μm were used as efficient photoabsorber by Warren *et al.*[14]. The orthogonal light absorption and the radial diffusion of photogenerated minority carriers in microstructured pillars have been demonstrated to efficiently increase the photocurrent density of microstructured Si[15]. Nevertheless, the microstructuring also increases the surface area of the photocathode. Therefore, increase in photocurrent density in case of SiMPs samples could be due to the higher light absorption efficiency and larger surface area for water reduction reaction. In case of the 5μm sample the photocurrent density is lower due to the thicker initiation layer that hinders the transfer of photogenerated minority carriers to the electrolyte. To check the influence of the SiO_2 layer covering the SiMPs, we compared the behavior of the 22μm thick film with and without HF etching. After the removal of the SiO_2, stated by the XPS analysis, the saturation current density increased from 24 to 30mA/cm^2, and the onset moved further into anodic direction (Fig. 4(b)).

Dai *et al.*[16] have shown that a Si nanowire with 1nm thin layer of SiO_2 exhibits higher photoelectrochemical performance than nanowire with thicker SiO_2 layer on it. A possible explanation for this result is that, due to the removal of the SiO_2 layer from the SiMPs photocathode, the photogenerated electrons can move to the electrolyte surface with a reduced recombination probability, producing a higher photocurrent as well as the shift of the onset potential in anodic direction.

According to the study of Warren *et al.*, SiMPs of 100mm height can absorb and convert 90% of the incident light[14]. In our study the photocurrent density of 40μm shows a value of 37.5mA/cm^2 but the onset potential (the voltage where the photocurrent is stronger than the dark current) shifts towards cathodic direction in comparison to the 22μm sample. This indicates that the increase of the micropillars height increases the absorption of photons and gives rise to the higher photocurrent density. On the other hand, in 40μm SiMPs sample the onset potential shifts towards cathodic direction, i.e a higher applied potential is needed to get H_2 from electrolyte. The shift in the onset potential towards cathodic direction for the 40μm could be due to the formation of larger semiconductor-electrolyte junction area that shifts the onset potential unfavorably[2,17,18].

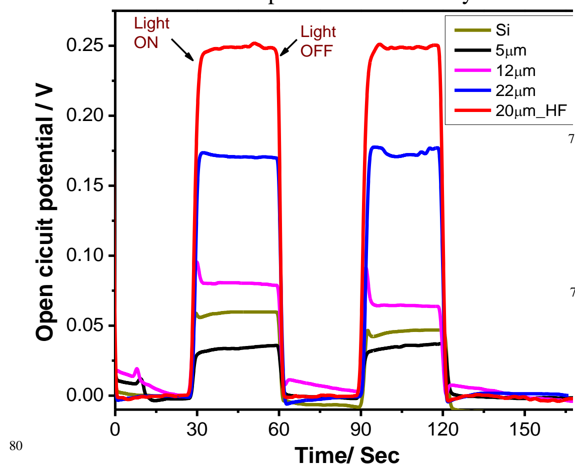

Fig. 6 Open circuit potential in dark and light in 30sec intervals for planar Si and SiMPs sample of different thicknesses as labeled in the graph. The sample 22μm_HF corresponds to the etched 22μm sample.

Table 1 Open circuit potential, onset potential at 1mA/cm^2 current density and saturation current density of Si and SiMPs samples of different thickness and 22μm sample etched with HF.

sample	OCP (V vs RHE)	On set pt. at -1mA.cm^{-2} (V/RHE)	Saturation current density mA.cm^{-2}
Si	0.080	-0.341	21
5μm	0.034	-0.390	17
12μm	0.080	-0.328	24
22μm	0.170	0.090	24
22μm_HF	0.245	0.134	30

[a] Footnote text.

The shift of the onset potential in the SiMPs samples shows that not only the absorption of incident photon but also the electrochemical performance gets better than in planar Si photocathode. In fact, the shift of onset potential does not depend on the absorption efficiency, but rather depends on the amount of photovoltage generated by the photoelectrodes. Due to the microstructuring the surface area of the photocathode increases and produces more sites for chemical reaction to occur which cause in the shift in onset potential [11]. The microstructures have also higher roughness than the planar Si and with the increase in roughness the reaction sites also increase which may result in increase of photovoltage and hence the shift in onset potential of the SiMPs [22]. To determine the amount of photovoltage generated by the photocathodes, we measured the open circuit potential (OCP) under illumination, as shown in Fig. 6. The OCPs of the

Nanoscale Accepted Manuscript

This journal is © The Royal Society of Chemistry [year]

photocathodes are 0.034, 0.060, 0.080, 0.170 and 0.240V for, respectively, the 5µm, planar Si, 12µm, 22µm, and 22µm_HF (HF treated) photocathodes. The photovoltage is determined by the generation of minority charge carriers and their movement towards the semiconductor/electrolyte interface under illumination due to the generation of minority charge carriers and their movement to the electrolyte. It is already theoretically demonstrated by Walter et al. the orthogonal absorption of the light bye the microstructure and less distance travel by the minority charge carrier before recombination enhances the open circuit potential [18]. In the present study the microstructures have diameter close to the theoretical value 1 µm. Therefore the collective effect of lower surface reflectance and shorter distance for minority charge carrier to react increases the OCP and hence the onset potential at 1mA/cm^2 shifted by ~400mV for SiMPs compared to planer Si photocathodes.

In Table 1 the OCPs, onset potentials, and the saturation current densities of the investigated samples are summarized. For higher OCP the shift in the onset of the photocurrent is higher.

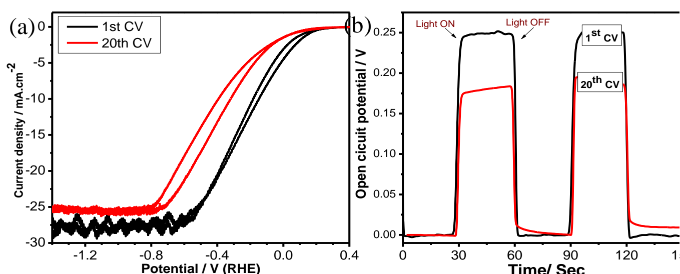

Fig. 7 The 1st and 20th cyclic voltametry (CV) curves of SiMPs 22µm samples etched with HF with light irradiated (a). OCP after 1st and 20th CV cycle (b).

The microstructuring results in higher OCP with the exception of the 5 µm thick SiMPs. The maximum OCP obtained for planar Si and Si wire with n$^+$-p junction are 0.56 and 0.54V [19]. The increase of the OCP of SiMPs photocathodes reflects the onset shifts towards more anodic direction in the j-V. PEC devices have the problem of the stability of the photoelectrode. An efficient photoelectrode must be stable under cyclic operation as well as in photoelectrochemical media. To study the stability we perform the repeated cyclic voltammetry test under illumination of light. In Fig. 7(a), the 1st and 20th CV cycle under illumination are shown for the SiMPs sample etched with HF (20 µm_HF). Just after 20 cycles the onset potential shifts towards cathodic direction by 130mV and the current density also decreases from 29 to 25mA/cm^2. On careful analysis we can see that the slope of the CV also changes after 20 cycles and this shows that the reaction kinetics also changes with cycling. Although the operating potential is in cathodic direction there may not be oxidation due to the applied potential but the Si surface is immerged in the electrolyte and the evolution of H_2 also produces O_2 that can react with the Si surface to oxidize it. In addition, the OCP dropped down from 249 to 180mV between the 1st and 20th CV loop (Fig. 7(b)). The aforementioned results show a quick degradation of SiMPs photocathodes only after 20 cycles of CV. The decrease in photocurrent density and the shift in onset potential towards cathodic direction are related to photogenerated charge separation at the electrode-electrolyte interface. The decrease in PEC performance of the photocathode could be due to the formation of a thicker SiO_2 layer on micropillars. For the stable performance of the photocathodes the SiMPs surface must be modified to check further oxidation.

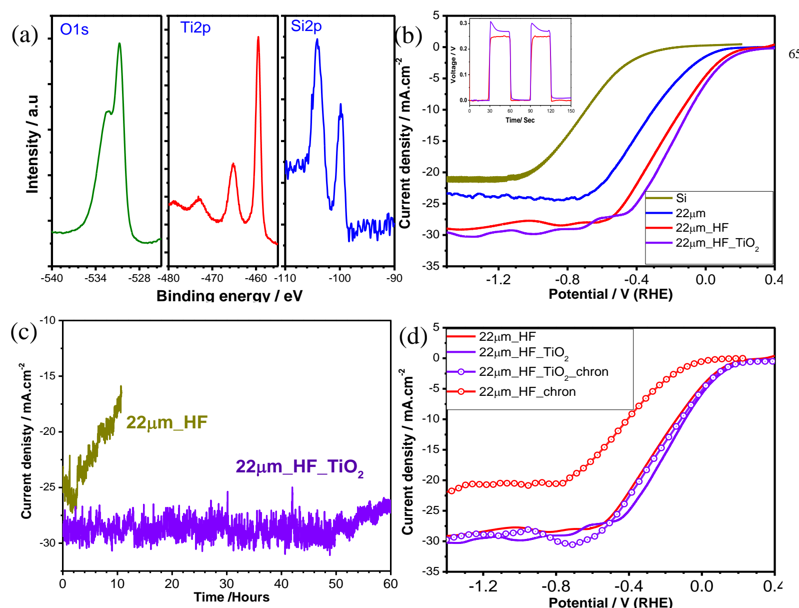

Fig. 8 O1s, Ti2p and Si2p XPS spectra of the TiO_2/SiMPs sample (a), j-V characteristics of the TiO_2 coated SiMPs in comparison to the bare SiMPs (b), chronoamperemetry test of TiO_2 coated and bare SiMPs sample at -0.8V of applied (c) and the j-V curve before and after 10h of chronoamperometry test (d). In the latter the curves with circles joined with line shows the j-V curve after chronoamperometry test.

Nanoscale Accepted Manuscript

Cite this: DOI: 10.1039/c0xx00000x

www.rsc.org/xxxxxx

ARTICLE TYPE

The SiMPs surface can be protected by laminating a conducting layer on it. Here, we use atomic layer deposition technique to deposit a very thin film of TiO_2 (4nm) on top of the SiMPs (22 µm_HF sample was chosen as it showed the best PEC performance). XPS spectra of the Ti2p, O1s and Si2p core levels, shown in Fig. 8(a), confirm the successive deposition of TiO_2 on SiMPs. The peak at 460eV in the Ti2p core level spectrum corresponds to the Ti^{4+} states, and the O1s peak at 530eV corresponds to oxygen bonded to Ti atom. But in O1s spectra a shoulder at higher binding energy at 533.4eV comes from O-Si bond. The presence of SiO_2 can be observed also in the Si2p spectra shown in Fig. 8(a). The peak in the Si2p spectrum at 104.1eV corresponds to Si^{4+} and the peak at lower energy at 99.7eV is attributed to Si^0. The Si^{4+} peak has higher intensity than the Si^0 peak, this means that the SiMPs sample is covered with a thin layer of SiO_2.The formation of SiO_2 on SiMPs sample may come from two routes; (1) micro- or nanostructure Si has high tendency to react with ambient atmosphere to form SiO_2 and (2) during the ALD processing the Si surface also reacts with the precursor and water to form a thin layer of SiO_2. The electrochemical performances of the TiO_2 coated SiMPs samples are shown in Fig. 8(b). After the deposition of TiO_2 onto the SiMPs sample the electrochemical performance show a very little change in the onset potential but the photocurrent density remains the same. The OCP of the TiO_2 coated SiMPs is about 20mV higher than that of bare SiMPs samples (inset in Fig. 8(b)). This increase of the OCP results in a shift of the onset potential in more anodic direction by about 30mV compared to the SiMPs sample. The shift in onset of the TiO_2 laminated SiMPs could be related to the surface passivation effect of TiO_2 as are result of which the charge carriers at Si-electrolyte surface separate very easily without excessive recombination.

The photoelectrochemical stability of the TiO_2 coated and bare SiMPs samples are checked by the chronoamperometry test under illumination at applied potential of -800mV (RHE) and the result is shown in Fig. 8(c). In case of bare SiMPs the current density remains constant within the noise signal for 2h of illumination and then it starts to decrease gradually. After 10h of illumination, the current density of bare SiMPs decreased from 28 to 20mA/cm^2. On the other hand the SiMPs sample coated with TiO_2 shows considerable stable current density of 30mA/cm^2 for 3.5h and then a small fluctuation is observed. Unlike the bare SiMPs, the decrease in photocurrent density is slow in case of TiO_2 coated SiMPs samples where the value changes from 30 to 28mA/cm^2 after illumination in electrochemical medium for 60h. The thin and compact film of TiO_2 deposited by ALD does not allow the SiMPs to be in direct contact with the electrolyte. Due to its high optical band gap (~3.2eV) TiO_2 can only absorb the UV region of light and the rest of the radiation in the non-UV spectral region can pass the TiO_2 layer[20]. Moreover the thickness of TiO_2 here is about 4nm and hence the TiO_2 cannot effectively absorb light. So the coating of the SiMPs with TiO_2 does not compromise the optical property of the SiMPs photocathode. The onset potential and the current density show that the TiO_2 did not negatively affected the electrical property of the SiMPs sample. The photogenerated minority charge carriers move across the thin film of TiO_2 to the electrolyte to perform the chemical reaction. The protections of Si against photoelectrochemical corrosion have been studied by using insulating Al_2O_3 [21], conducting graphene layer[22], and semiconducting TiO_2 layers [23]. In case of Al_2O_3 the limiting thickness for photogenerated electron to be transferred to the electrolyte is 4nm since the Al_2O_3 is insulating and the charge carrier has to tunnel through this layer. On the other hand while using TiO_2 prepared by ALD the thickness of TiO_2 can go up to more than 40nm since this layer is amorphous and carries a high conductivity. In our study, the TiO_2 grown by ALD is amorphous [24] so it has higher conductivity than the crystalline TiO_2. The ALD layers facilitate the easy flow of charge carriers across the Si/TiO_2 interface and protect the Si surface against direct contact to the electrolyte. Therefore, after electrochemical dissociation of the electrolyte the H_2 and O_2 will not be in direct touch with Si and none of them can interact with Si to decrease the photoelectrochemical property of the photocathode.

In Fig. 8(d) the j-V characteristic before and after 10h of chronoamperometry test is shown. The bare SiMPs shows a considerable decrease in the photocurrent density as well as a shift of the onset potential towards cathodic direction; the corresponding values are 21mA/cm^2 and 80mV shift, respectively. These changes reflect degraded charge separation ability and catalytic activity of the based PEC devices. In contrast, when the SiMPs is coated with TiO_2 layer the change in current density is not visible and there is a smaller shift in the onset potential compared to bare the SiMPs by about 15mV towards cathodic direction. Thus, the conducting layer of TiO_2 protect against photocorrosion of SiMPs as well as against degradation of electrocatalytic properties.

Basing on the results shown in Fig. 8, we suppose that the TiO_2 has a little passivation effect on the performance of SiMPs. However, the chronoamperometry test indicates that the overlayered TiO_2 on the SiMPs protects against corrosion very effectively whereas its effect on surface passivation is comparatively weak.

Conclusions

In this study, we use Si microstructures as very promising candidates for the photocathodes for water splitting application. These structures can be obtained in low-cost processes and, in addition, can be used without any additional catalysts. This process of Si microstructure preparation can be controlled to obtain SiMPs with different thickness.

The as grown Si microstructures were covered with a thick (155nm) SiO_2 layer which, as we have shown, can be removed by

Nanoscale Accepted Manuscript

appropriate etching.

The microstructured Si is in two ways beneficial for photocathode applications in water splitting devices. It not only increases the photocurrent density but also shifts the onset potential in anodic direction without any catalyst. The shift of onset potential is related to the generation of higher photovoltage in microstructures when compared to planar Si. However, the microstructured Si itself shows no long-time stability when used for photocatalytic water splitting.

Therefore, we used ALD technique to deposit TiO_2 homogenously on these microstructures. The TiO_2 grown by ALD at 250 ℃ yields a film thickness of 4nm. It has a positive effect on the onset potential and we have seen that the onset of TiO_2 coated SiMPs shifts further towards anodic direction. Obviously, the shift is due to a better charge separation across the Si/TiO_2 interface than across the Si/SiO_2 interface. We could demonstrate in addition that the thin ALD-TiO_2 layer has a considerable improved long-term stability (over 60h of illumination) and we find no significant change in the electrochemical properties of the electrodes. Moreover, using conformal ALD-TiO_2 thin films the Si microstructures can be protected against oxidation.

Although, the TiO_2 overlayer has been intensively studied for the stability of photoelectrodes, ([23,25]) it was not investigated yet to block the surface oxidation of SiMPs. The TiO_2 layer here was used to control the SiO_2 thickness on SiMPs which has an effect on the photocatalytic activity of the SiMPs photocathodes.

Acknowledgements

We acknowledge K. Kędzierski, Faculty of Technical Physics, Poznan University of Technology, for reflectance measurement and discussion of data . We acknowledge K. Henkel, U. Kramm, G. Beuckert and M. Sowinksa for the discussion and providing support for experiments. We would like to acknowledge the German Research Foundation (DFG SCHM 745/31-1) and international graduate school at Brandenburg University of Technology Cottbus-Senftenberg for funding.

Notes and references

[a] *Brandenburg University of Technology, Panta Rhei K.-Wachsmann-Allee 17, Cottbus, Germany. Fax: +49 (0)355-69-3931; Tel: +49 (0)355-69-2999; E-mail: chittaiit@yahoo.com*

1 J. R. Bolton, S. J. Strickler and J. S. Connolly, Nature. 1985, **8**, 495.
2 S. Fukuzumi, D. Hong and Y. Yamada, J. Phys. Checm. Lett. 2013, **4**, 3459.
3 M. D. Kärkäs, O. Verho, E. V. Johnston and B. Åkermark, Chem. Rev. 2014, **114**, 11863.

5 C.Das, K. Henkel, M. Tallarida, H. Gargouri, I. Kärkkänen, J. Schneidewind, B. Gruska, M. Arens and D. Schemeisser, J. Vac. Sci. Technol. A 2015, **33**, 01A144.
6 *D.* Barreca, G. Carraro, A. Gasparotto, C. Maccato, F. Rossi, G. Salviati, M. Tallarida, C. Das, F. Fresno, D. Korte, U. L. Stangar, M. Franko and D. Schmeißer, ACS Appl. Mat. & Int. 2013, **5**, 7130.
7 L. L. Ma, Y. C. Zhou, N. Jiang, X. Lu, J. Shao, W. Lu, J. Ge, X. M. Ding, and X. Y. Hou, *J. Appl. Phys. Lett*. 2006, **88**, 171907.
8 H.S. Seo, X. Li , H.D. Um, B. Yoo, J.H. Kim, K.P. Kim, Y.W. Cho and J.H. Lee, *Mat. Lett.* 2009, **63**, 2567.
9 Z.H. Lu, M.J. Graham, D.T. Jiang and K.H. Tan, *Appl. Phys. Lett.* 1993, **63**, 2941-2943.
10 A. Verdaguer, C. Weis, G. Oncins, G. Ketteler, H. Bluhm and M. Salmeron, *Langmuir* **2007**, 23, 9699-9703.
11 J. Oh, T. G. Deutsch, H.-C. Yuan and H. M. Branz, *Energy Environ. Sci.* 2011, **4**, 1690.
12 E. Garnett and P. Yang, *Nano Lett*. 2010, **10**, 1082.
13 C. Battaglia, C.-M. Hsu, K. Söderström, J. Escarré, F.-J. Haug, M. Escarrè, M. Boccard, M. Despeisse, D. T. L. Alexander, M. Cantoni, Y. Cui and C. Ballif, *ACS Nano*, 2012, **6**, 2790.
14 E. L. Warren, S. W. Boettcher, J. R. McKone and N. S. Lewis, *Proc. of SPIE*. 2010, **7770**, 77701F-7.
15 B. M. Kayes, H. A. Atwater and N.S. Lewis, *J. Appl. Phys.* 2005, **97**, 114302.
16 P.Dai, J. Xie, M. T. Mayer, X. Yang, J. Zhan, and D. Wang, Angew. Chem. Int. Ed. 2013, **52**, 11119.
17 Kayes, B. M.; Atwater, H. A.; Lewis, N. S.; *J. Appl. Phys.* **2005**, 97, 114302-11.
18 M. G. Walter, E.L. Warren, J.R. McKone, S.W. Boettcher, Q. Mi, E.A. Santori and N.S. Lewis, *Chem. Rev*. 2010, **110**, 6446.
19 S. W. Boettcher, E. L. Warren, M. C. Putnam, E. A. Santori, D. T. Evans, M. D. Kelzenberg, M. G. Walter, J. R. McKone, B. S. Brunschwig, H.A. Atwater and N. S. Lewis, *J. Am. Chem. Soc.*, 2011, **133**, 1216.
20 U.Diebold, Sur. Sci. Rep. 2003, **48**, 53.
21 M. Choi, J. Y. Jung, M. J. Park, J. W. Song, J. H. Lee and J. H. Bang, J. Mater. Chem. A. 2014, **2**, 2928.
22 U. Sim, T. Y. Yang, J. Moon, J. An, J. Hwang, J. H. Seo, J. Lee, K. Y. Kim, J. Lee, S. Han, B. H. Hong and K. T. Nam, energy Environ. Sci. 2013, **6**, 3658.
23 S. Hu, M. R. Shaner, J. A. Beardslee, M. Lichterman, B. S. Brunchwig and N. S. Lewis, Science 2014, **344**, 1005.
24 C. Das, M. Tallarida, D. Schmeisser, Environ. Earth Sci. 2013, **70**, 3785.
[25] B. Seger, T. Pedersen, A. B. Laursen, P. C. K. Vesborg, O. Hansen and I. Chorkendroff, J. Am. Chem. Soc. 2013, **135**, 1057

Nanoscale Accepted Manuscript